Chemical Physics 409 (2012) 74–78

Contents lists available at SciVerse ScienceDirect

Chemical Physics

journal homepage: www.elsevier.com/locate/chemphys

Comment

Theoretical reproduction of superstructures revealed by STM on bilayer graphene

E. Cisternas [a,*], J.D. Correa [b]

[a] Departamento de Ciencias Físicas, Universidad de La Frontera, Casilla 54 D, Temuco, Chile
[b] Departamento de Ciencias Físicas, Universidad Andres Bello, Av. República 220, 837-0134 Santiago, Chile

ARTICLE INFO

Article history:
Received 19 April 2012
In final form 20 September 2012
Available online 9 October 2012

Keywords:
Bilayer graphene
Superstructures
STM

ABSTRACT

We performed density functional theory calculations and we calculated Scanning Tunneling Microscopy images (constant height mode) on twisted bilayer graphene (BLG). The STM theoretical images show the graphene structure and also superstructures. The roughness associated to the surface carbon atoms appears over a large oscillation amplitude which is in agreement with the "giant corrugation" experimentally reported by several authors. Additionally we found a strong dependence between the corrugation amplitude of the calculated images and the bias voltage considered. These results suggest that superstructures in twisted BLG have to do mainly with a redistribution of the electronic density and that deformations introduced by tip-sample mechanical interaction could be of second order.

1. Introduction

The increasing interest on nanoscience and nanotechnology has evidenced the importance of the scanning tunneling microscope (STM) to explore the nature at atomic scale. In this context graphene, a novel layered material with potential technological applications [1], has been intensively characterized by STM techniques and has revealed a surprising behavior: edge states at layer borders [2,3], superstructures [4–6] and Van Hove Singularities [7]. These particularities were evidenced from STM characterizations of highly oriented pyrolitic graphite (HOPG) since the difficulties to obtain full atomic resolution and the observation of superstructures gave the first signals of the poor understanding of the electronic structure of the layers.

To extend the preceding statements, let us precise that graphene is a stable bi-dimensional structure formed by carbon atoms ordered in a hexagonal lattice (the first neighbor distance is 1.42 Å). In crystalline graphite (HOPG) such layers are stacked on each other in a *AB* sequence, which means that it is possible to identify two type of atomic sites: the α-type, corresponding to atoms with neighbors directly above and below in adjacent layers; and the β-type, which do not have direct neighbors in the adjacent layers. An important consequence of the crystalline structure of HOPG is that near the Fermi level the bulk presents a Local Density of States (LDOS) which is larger for atoms on β-type sites [8]. Thus, as the accessible states for STM are those in the energy window $[E_{Fermi} - eV_{bias}, E_{Fermi}]$ [9,10], only those atoms on β-type sites appears visible for a STM which operates at low bias voltage. These atomic sites give rise to the triangular lattice which is usually reported on STM experiments. However, as experimental STM images show triangular structures even for a wide range of bias voltages, the persistence of the triangular lattice has been explained considering resolution losses introduced by the STM tip size [11].

Following the preceding ideas, the observation of superstructures during STM experiments can be explained by considering a rotations among graphene layers. Such rotations generate the well known *Moiré Patterns*: interference patterns whose origin is the mismatch between two periodic lattices. In the graphene case it is possible to identify regions with high concentration of β-type sites, called g–β sites, and regions with high concentration of α-type sites, called g–α sites or *AA* stacking regions [see Fig. 1(a)]. In both cases g stands for *giant* [12]. In the frame of the explanation of Tománek and Louie [8], and due to the large LDOS of atoms on β sites [12], the g–β regions would present the current intensity maxima in STM images acquired at low bias voltages. However, Rong and Kuiper [13] based on first-principles DOS calculations [14], proposed that current maxima occur over g–α regions. Additionally a third explanation for the superstructures considers that surface deformations introduced by STM tip (see Ref. [15] and references therein) could explain the observation of superstructures, instead of electronic effects induced by rotation between weakly interactive graphene layers. This has been a long standing controversy which has attracted renewed attention over the STM image formation of graphite surface [11,16–18] and over the physical origin of superstructures [15,19–21], due to the increasing interest on graphene.

In this context, an important tool to analyze the effect of rotation among graphene layers is the calculation of STM images and

* Corresponding author.
E-mail address: eduardo.cisternas@gmail.com (E. Cisternas).

0301-0104/$ - see front matter © 2012 Elsevier B.V. All rights reserved.
http://dx.doi.org/10.1016/j.chemphys.2012.09.021

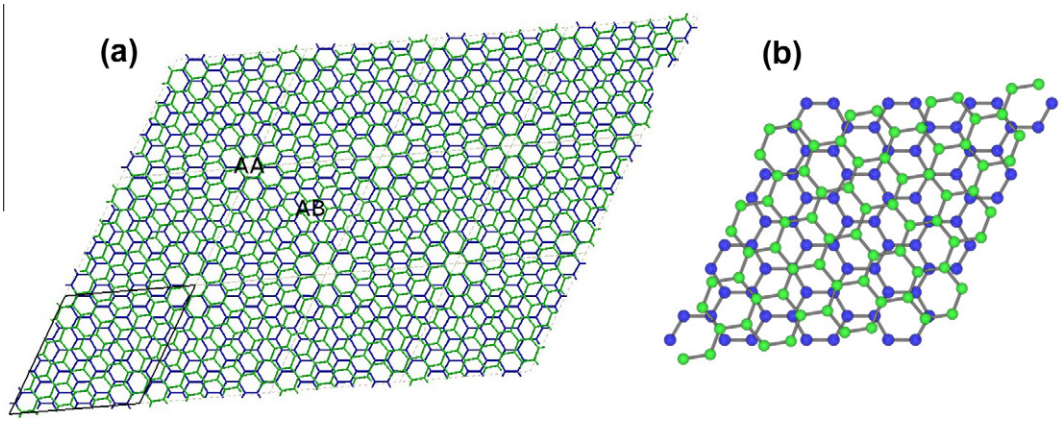

Fig. 1. (a) Scheme view of twisted bilayer graphene for 7.3° as rotation angle. (b) Magnification of the unit super-cell which expands the superstructure. Top layer was colored green and bottom layer in blue. (For interpretation of the references to colour in this figure legend, the reader is referred to the web version of this article.)

the corresponding contrast with experimental data. Following this objective we have focused in the task of calculate STM images for different rotation angles between two graphene layers and study the influence of experimental parameters as bias voltage and tip-surface distance. We have organized this paper as follows: details of the images calculation are given in next section; theoretical results are summarized in Section 3 and finally appear the main conclusions.

2. Calculation method

The system under study corresponds to BLG presenting a relative rotation angle between its layers (twisted bilayer graphene). Rotations occur around the stacking direction and despite for any angle one can identify a superstructure (or Moiré Pattern) only for very particular angles the misoriented layers are in commensuration [21–23]. A commensurable unit super-cell requires a rotation from a vector $\vec{V}_1 = m\vec{a}_1 + n\vec{a}_2$ to $\vec{V}_2 = n\vec{a}_1 + m\vec{a}_2$, where $\vec{a}_1 = (\sqrt{3}, -1)a_0/2$ and $\vec{a}_2 = (\sqrt{3}, 1)a_0/2$ are the graphene basis vectors; m and n are integers and $a_0 = 2.46$ Å is the lattice constant. The commensurable rotation angle is defined by

$$\cos\theta = \frac{m^2 + 4mn + n^2}{2(m^2 + mn + n^2)} \tag{1}$$

and the unit super cell vectors correspond to: $\vec{t}_1 = \vec{V}_2 = n\vec{a}_1 + m\vec{a}_2$ and $\vec{t}_2 = -\vec{a}_1 + (m+n)\vec{a}_2$ [21]. The unit super-cell contains $N = 4(m^2 + mn + n^2)$ atoms and its periodicity results $D = a_0/[2\sin(\theta/2)]$ [12,15]. Thus, commensurable unit super-cells are completely defined by the index m and n and those selected for this study appear in Table 1 with their corresponding number of atoms (N), rotation angle between layers (θ) and periodicity (D). For example, the unit super-cell for twisted bilayer graphene with the angle 7.3° is shown in Fig. 1(b).

Our DFT calculations were carried out using the SIESTA ab initio package [33] which employ norm-conserving pseudo-potentials and localized atomic orbitals as basis set. Double-ζ plus polarization functions were used under the local density approximation [34]. All structures were fully relaxed until the atomic forces are smaller than 0.02 eV/Å. We consider super-cells with periodic boundary conditions for the plane layers, while in the perpendicular direction to the layers plane the separation between slabs is fixed to 14 Å. The Brillouin zone sampling was performed using a Monkhorst–Pack mesh of $10 \times 10 \times 1$.

The images were obtained using the code *STM* 1.0.1 (included in the SIESTA package). This code uses the wave functions generated by SIESTA and computed on a reference plane and extrapolates the value of these wave functions into vacuum. Such reference plane must be sufficiently close to the surface so that the charge density is large and well described. The STM data is generated under the Tersoff–Hamann theory [9], while data visualization was possible using the WSxM 5.0 freeware [35]. A Gaussian smoothing was performed to obtain the final STM image.

Table 1
Selected commensurable unit super-cells and their corresponding number of constituent atoms (N), rotation angle (θ) and periodicity (D). The last column shows periodicities experimentally reported.

m	n	N	θ	D (nm)	D Exp. (nm)	
2	1	28	21.8°	0.65	0.65 Ref. [24]	
3	2	76	13.2°	1.05	1.06 Ref. [25]	0.95 Ref. [26]
4	3	148	9.4°	1.50	1.50 Ref. [27]	1.50 Ref. [28]
5	4	244	7.3°	1.91	1.76 Ref. [29]	1.71 Ref. [30]
6	5	364	6.0°	2.30	2.20 Ref. [31]	2.40 Ref. [32]

3. Results

Electronic properties and constant height mode STM images were calculated for the five commensurable super-cells presented in Table 1. Fig. 2 shows band structure and total density of states (DOS) for three of these twisted bilayer graphene. Clearly, a decrease of the rotation angle θ diminishes the energy difference between the VHS near the Fermi Level. This effect was reported in previous works [7,21,36] and has its origin in the renormalization of Dirac electrons velocities, which is observed in the band structures as a decreasing in the slope of the Dirac cone. Additionally the VHSs show the well known asymmetry between electrons and holes, which is observed as a difference in the height of the VHSs. These theoretical predictions have been recently corroborated by STM/STS experimental measurements on twisted graphene layers with $\theta = 1.79°$ [7] and they ensure us that we reproduce the main electronic characteristics of the twisted bilayer graphene.

The energy window $[E_{Fermi} - e|V_{bias}|, E_{Fermi}]$ contains the occupied states contributing to the STM image [9,10]. Thus, the influence of bias voltage dependence was studied considering several values in the interval $0.05\,V < V_{bias} < 3.0\,V$. As example, Fig. 3 shows STM images, which were calculated with the parameters $V_{bias} = 1.0$ V and tip-to-surface distance $d_{TS} = 1.0$ Å. Each image shows current intensity maxima zones (brilliant) forming triangular structures. The lattice constants of these triangular structures correspond to the periodicities D shown in Table 1, and they are commonly known as *super-lattice constants*.

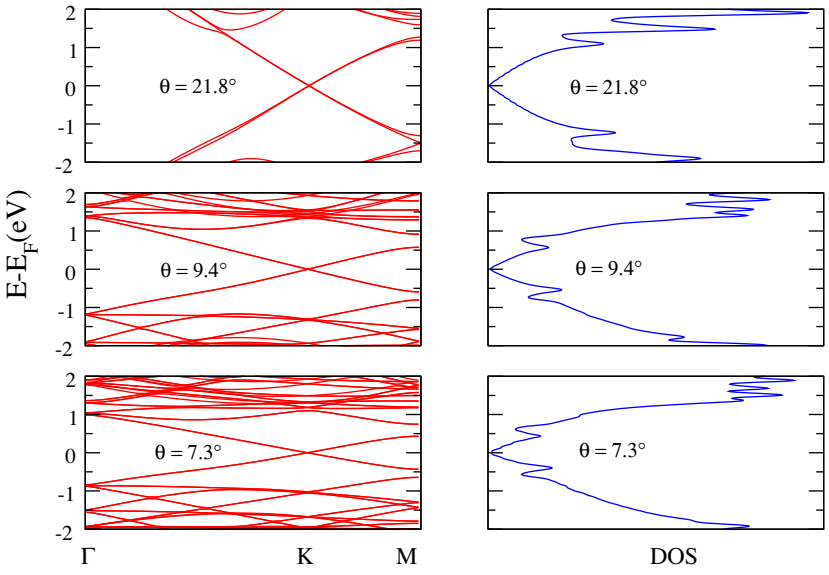

Fig. 2. Bands structure and total density of states for different twisted bilayer of graphene. Left panels show the bands structures and right panels show the total density of states.

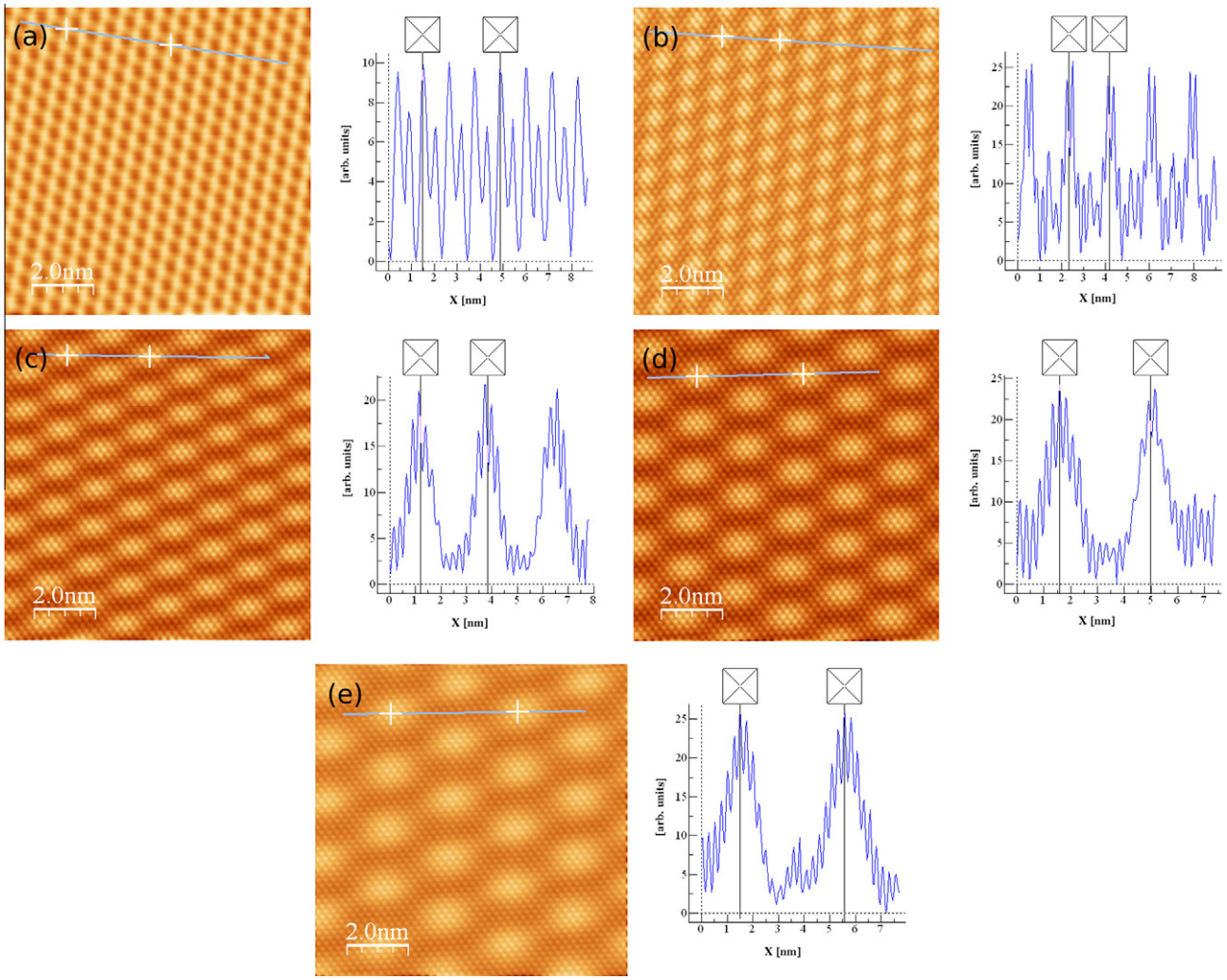

Fig. 3. STM images calculated for the five commensurable unit super-cells presented in Table 1. Line profiles along the indicated segment appears at right of each image.

These calculated STM images also show that brilliant zones lay over regions with *AA* stacking. This observation is in accordance with the conclusions of other authors: Rong and Kuiper [13] and Campanera et al. [19], who based their conclusions in DOS obtained ab initio for different stacking sequence of graphite [14]; and Trambly de Laissardiere et al. [21], who combined tight-binding and ab initio calculations to study the LDOS on twisted bilayer graphene.

Line profiles were performed along the segment indicated in each STM image of Fig. 3. Although the calculated images correspond to constant height mode (CHM), the line profiles might be compared with those experimentally obtained in constant current mode (CCM) by assuming that depressions in current intensity in CHM lead to proportional approximations of the tip-to-the-surface in CCM in order to keep the tunnel current constant. So, our results show two important features which have been revealed also during STM experiments: a roughness presenting the graphite periodicity and a large oscillation amplitude with the super-lattice periodicity [12,13,15]. The roughness reflects the electronic charge accumulation at atomic sites and, as the oscillation amplitude is much more larger than the atomic sites roughness, experimental physicists have named it "giant" or "super-lattice corrugation" [15].

Also we found, coinciding with experimental observations on graphite surface [13,15], a strong influence of bias voltage over the *super-lattice corrugation amplitude* (SLCA). Graphically this behavoir is shown in Fig. 4: the SLCAs for the five super-cells are shown as a function of the bias voltage considered to calculate it. Thus, for $\theta = 21.8^\circ$ we found that a SLCA maximum appears for $V_{bias} \approx 1.0$ V which is coincident with the first VHS occuring at ≈ -1.0 V (see Fig. 2). This fact indicates that the main contribution to this VHS comes from the Local Density of States (LDOS) over the *AA* stacking regions and, as a consequence, a STM operating at this bias voltage will reveal the superstructure. As counterpart, the decrease of the SCA for $V_{bias} > 1.0$ V shows that the resting stacking regions start to contribute strongly to the total DOS, therefore for a STM operating at such bias voltage will be difficult to reveal a superstructure. A similar analysis can be done for $\theta = 9.4^\circ$: its first VHS occurs at $V \approx -0.5$ V and its corresponding SLCA increases notoriously for $V_{bias} \approx 0.5$ V. In this case the SLCA reaches a maximum at $V_{bias} \approx 1.5$ V, coinciding with the second VHS, and then decreases rapidly. Again this fact indicates that the third VHS has contributions from the LDOS of the different stacking regions. When $\theta = 7.3^\circ$, the first VHS at $V \approx -0.5$ V is reflected in the noticeable increasing of the corresponding SLCA. However when the bias voltage increases over 2.0 V the LDOS from other regions start to contribute equally to the total DOS and the SLCA starts to diminish. The LDOS behavior has been experimentally revealed by STS on the bright and dark regions of STM data [7,24].

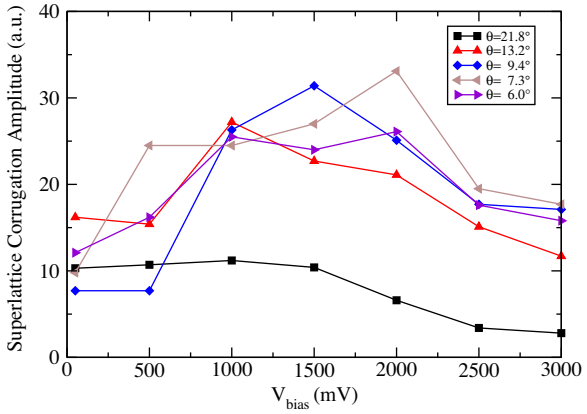

Fig. 4. Super-lattice Corrugation Amplitude on calculated STM images as a function of bias voltages. The rotation angles for the twisted BLG are indicated in the figure.

On the other hand the STM image dependence on the tip-to-sample distance (d_{TS}) was also studied by considering different values in the range 1.0 Å $< d_{TS} <$ 2.0 Å. For larger d_{TS} we could not obtain STM images with enough reliability. Nevertheless, the methodology used in this study to generate STM images shows that the tip-to-surface distance variations have no relevant consequences in the calculated STM images and, besides, the current intensity maxima remain over the regions with large concentration of α-sites (*AA* regions). This confirms that the present methodology to obtain STM images is well defined for the range d_{TS} considered, but does not give definitive conclusions about tip-to-sample distance dependence as those experimentally observed [6] and that we have theoretically predicted for $d_{TS} >$ 2.0 Å [20] in trilayer graphene with the surface layer rotated by 21.8°.

4. Conclusions

Using ab initio methods we have calculated STM images, corresponding to constant height operation mode, for twisted graphene bilayers presenting distinct commensurable rotation angles. These calculated images show superstructures whose morphology and periodicity present a remarkable agreement with experimental observations. Thus the line profiles obtained from the calculated images, show oscillation amplitude (giant corrugation) with the periodicity of the superstructures which is notably more larger than the roughness associated to the graphene lattice periodicity. Both characteristics have been experimentally observed and these theoretical results show that they have a strong electronic origin. As a consequence we suggest that mechanical tip-sample interaction, as well other physical grounds, could be of second order.

Three important additional remarks must be stated: first, despite the weak inter-layer interaction between graphene layers, a misorientation between them can modify considerably the electronic structure of the surface; second, results show clearly that, for twisted bilayer graphene, the current intensity maxima appear over *AA* stacking regions; and third, the bias voltage has a strong influence in the *super-lattice corrugation amplitude*.

Acknowledgements

This work was partially supported by Universidad de La Frontera, under Project DI11-0012. J.D.C. acknowledges FONDECYT postdoctoral program under Grant No. 3110123. We thanks Centro de Modelación y Computación Científica (CMCC), Universidad de La Frontera, by computational facilities and programing help. Dr. Marcos Flores is gratefully acknowledged for useful discussions.

References

[1] A.K. Geim, K.S. Novoselov, Nat. Mat. 6 (2007) 183.
[2] Y. Kobayashi, K. Fukui, T. Enoki, K. Kusakabe, Phys. Rev. B 73 (2006) 125415.
[3] Y. Niimi, T. Matsui, H. Kambara, K. Tagami, M. Tsukada, H. Fukuyama, Phys. Rev. B 73 (2006) 085421.
[4] M. Kuwabara, D.R. Clarke, D.A. Smith, Appl. Phys. Lett. 56 (1990) 2396.
[5] E. Loginova, S. Nie, K. Thürmer, N.C. Bartelt, K.F. McCarty, Phys. Rev. B 80 (2009) 085430.
[6] D.L. Miller, K.D. Kubista, G.M. Rutter, M. Ruan, W.A. de Heer, P.N. First, J. Stroscio, Phys. Rev. B 81 (2010) 125427.
[7] G. Li, A. Luican, J.M.B. Lopes dos Santos, A.H. Castro Neto, A. Reina, J. Kong, E.Y. Andrei, Nat. Phys. 6 (2010) 109.
[8] D. Tománek, S.G. Louie, Phys. Rev. B 37 (1988) 8327.
[9] J. Tersoff, D.R. Hamman, Phys. Rev. Lett. 50 (1983) 1998.
[10] A. Selloni, P. Carnevali, E. Tosatti, C.D. Chen, Phys. Rev. B 31 (1985) 2602.
[11] E. Cisternas, F. Stavale, M. Flores, C.A. Achete, P. Vargas, Phys. Rev. B 79 (2009) 205431.
[12] J. Xhie, K. Sattler, M. Ge, N. Venkateswaran, Phys. Rev. B 47 (1993) 15835.

[13] Z.Y. Rong, P. Kuiper, Phys. Rev. B 48 (1993) 17427.
[14] J.-C. Charlier, J.-P. Michenaud, X. Gonze, Phys. Rev. B 46 (1992) 4531.
[15] W.-T. Pong, C. Durkan, J. Phys. D: Appl. Phys. 38 (2005) R329.
[16] C.D. Zeinalipour-Yazdi, D.P. Pullman, Chem. Phys. 348 (2008) 233.
[17] G.S. Khara, J. Choi, J. Phys.: Cond. Matter 21 (2009) 195402.
[18] H.S. Wong, C. Durkan, N. Chandrasekhar, ACS Nano 11 (2009) 3455.
[19] J.M. Campanera, G. Savini, I. Suarez-Martinez, M.I. Heggie, Phys. Rev. B 75 (2007) 235449.
[20] E. Cisternas, M. Flores, P. Vargas, Phys. Rev. B 78 (2008) 125406.
[21] G. Trambly de Laissardière, D. Mayou, L. Magaud, Nano Lett. 10 (2010) 804.
[22] A.N. Kolmogorov, V.H. Crespi, Phys. Rev. B 71 (2005) 235415.
[23] S. Shallcross, S. Sharma, E. Kandelaki, O.A. Pankratov, Phys. Rev. B 81 (2010) 165105.
[24] A. Luican, G. Li, A. Reina, J. Kong, R.R. Nair, K.S. Novoselov, A.K. Geim, E.Y. Andrei, Phys. Rev. Lett. 106 (2011) 126802.
[25] B. Nysten, J.-C. Roux, S. Flandrois, C. Daulan, H. Saadaoui, Phys. Rev. B 48 (1993) 12527.
[26] J.C. Moreno-López, M.C.G. Passeggi Jr., J. Ferrón, Surf. Sci. 602 (2008) 671.
[27] V. Elings, F. Wudl, J. Vac. Sci. Technol. A 6 (1988) 412.
[28] I.K. Song, J.R. Kitchin, M.A. Barteau, Proc. Natl. Acad. Sci. 99 (2002) 6471.
[29] T.R. Albrecht, H.A. Mizes, J. Nogami, S. Park, C.F. Quate, Appl. Phys. Lett. 52 (1988) 362.
[30] K. Miyake, K. Akutsu, T. Yamada, K. Hata, R. Morita, M. Yamashita, H. Shigekawa, Ultramicroscopy 73 (1998) 185.
[31] T. Tanii, K. Hara, K. Ishibashi, K. Ohta, I. Ohdomari, Appl. Surf. Sci. 162 (2000) 662.
[32] Y. Yang, Ch. Bromm, U. Geyer, G. von Minnigerode, Ann. Phys. 1 (1992) 3.
[33] J.M. Soler, E. Artacho, J.D. Gale, A. Garcia, J. Junquera, P. Ordejón, D. Sánchez-Portal, J. Phys. Cond. Matter. 14 (2002) 2745.
[34] D.M. Ceperley, B.J. Alder, Phys. Rev. Lett. 45 (1980) 566.
[35] I. Horcas, R. Fernandez, J.M. Gomez-Rodriguez, J. Colchero, J. Gomez-Herrero, A.M. Baro, Rev. Sci. Instr. 78 (2007) 013705.
[36] E. Suárez-Morell, J.D. Correa, P. Vargas, M. Pacheco, Z. Barticevic, Phys. Rev. B. 82 (2010) 121407.